Appl. Sci. Converg. Technol. 25(5): 92-97 (2016)
http://dx.doi.org/10.5757/ASCT.2016.25.5.92

Research Paper

Practical Surface Sculpting Method for the Fabrication of Predefined Curved Structures using Focused Ion Beam

Heung-Bae Kim*
Department of Mechanical Engineering, Myongji College, Seoul 03656, Korea

Received July 12, 2016; revised August 9, 2016; accepted August 9, 2016

Abstract Surface erosion using focused ion beam irradiation is the most promising technology for the realization of micro/nanofabrication. However, accurate fabrication of predefined structures is still challenging. This article introduces a single step surface driving method to fabricated predefined curved structures. The previously reported multi step surface driving method (MSDM) has been modified so that a single ion dose profile can be used instead of multiple ion dose profiles. Experimental realization of the method is presented with the fabrication of predefined curved surfaces as well as reference to surface propagation theory. For the purpose of verification, simulations are performed on the basis of a sound mathematical model.

Keywords: Focused ion beam, Microfabrication, Nanofabrication

I. Introduction

The realization of complex three-dimensional (3D) structures in various materials at micro- and nano-meter scales is of great importance for a number of micromechanical, micro-optical and microelectronic applications. Especially, this is important for achieving functional integration in new and emerging products, such as biosensors, organic micro/nano-photonic systems and point-of-care diagnostic devices. Different lithographic techniques have been utilized to fabricate complex 3D structures, e.g. grey tone photolithography [1], electron beam lithography (EBL) [2], two-photon lithography [3], X-ray lithography [4], laser beam lithography [5] and nano-imprint lithography [6]. By employing these techniques, complex 3D shapes can be fabricated in resists. Subsequent pattern transfer from the structured resist to a wafer is performed via a dry etching process, such as ion milling, chemically assisted ion-beam-etching or reactive ion etching (RIE) [7]. An alternative technique is to use the patterned resist as a sacrificial template for producing metallic 3D masters through electroforming for serial replication by thermal imprinting/embossing or injection molding [8].

Focused Ion Beam (FIB) technology offers other possibilities for fabricating 3D micro- and nanostructures from almost any materials. This technology has attracted the attention of researchers due to its high patterning flexibility and sub 50 nm-resolution [9]. There have been a lot of efforts to find a way to fabricate predefined structures with good accuracy. However, a method for the accurate fabrication of material surfaces is still a challenge for various applications. Several remarkable efforts have been made to achieve those goals, including the Slice by Slice approach of Y. Fu et al. [10,11], the approach of variable pixel dwell time over the sample surface by Adams and Vasile et al. [12,13], and the Simulation based method, hereafter simply SBM, by Kim et al [14,15]. In the former two efforts, redeposition flux that is generated during the sputter process was not considered, while in the latter redeposition flux is automatically included during the simulation process. An accurate numerical scheme is necessary to fabricate arbitrary curved structures. The method must be simple and clear under surface propagation theory.

In this article, a single step surface driving method, hereafter referred to as SSDM (Single step surface driving method), which is modified from the previously reported multi step surface driving method (MSDM) [16], is introduced. Multiple calculation steps can be optimized and then it can be possible to utilize just one optimized ion dose profile. A discussion of SSDM will follow after the discussion of the previously reported accurate fabrication methods in Section II. We demonstrate and present the SSDM by realizing fundamental structures and verifying them with simulations.

II. Accurate Surface Fabrication Method

For simplicity of fabrication of the predefined structures, generally, two kinds of assumptions can be made. One is

*Corresponding author
E-mail: heungbaekim@gmail.com

the constant depth in sliced layers reported by Y. Fu [10, 11]; the other is the depth control by variable dwell time reported by Vasile [12,13]. In this section, these methods are introduced, as well as the multi step surface driving method (MSDM), in brief.

1. Depth control by variable dwell time approach

In the depth control by variable dwell time concept, Vasile and his coworkers used many different 3D structures to consider the sputter yield and changing dwell time at each pixel point over the substrate surface. Therefore, the milling depth is different for different pixel points. For each point, the required sputter yield as a function of the ion beam incident angle and dwell time were computed using a mathematical model. The whole process was controlled using an FIB-equipped computer language. Therefore, the method requires a long time and large computer space for the milling process. This cavity profile can be represented by a curve. The equation of the profile of the desired cavity is derived from the design. , and the milling process is divided into N steps. The desired parabolic trough cavity was obtained by milling the different sequential parabolic cavities to depths that get deeper from the top to bottom. Given the material parameters and the ion beam parameters, the dwell time at each pixel is solved to produce the milling depth, ΔZ; the depth increment needed at the (i, j) pixel can be expressed as

$$\Delta Z_{ij} = \iint \frac{\phi(x,y)}{\eta} f_{x,y}(x_i, y_j) S(\theta_{x_i,y_j}) t_{xy} dx dy \quad (1)$$

where $\Phi(x, y)$ is the ion flux at point (x, y), $ç$ is the atomic density of the target in atoms (cm^{-3}), $S(\theta x_i, y_i)$ is the angle dependent sputtering yield, t_{xy} is the dwell time of the ion beam at point (x, y) in units of seconds, and $f_{x,y}$ (x_i,y_i) is the ion beam density expressed as a Gaussian function in two dimensions.

The dwell time needed for the depth increment, through the intensity distribution, takes into account the contribution of the ion flux from all pixels on the deflection plane. The sputter yield is also adjusted point by point according to the change of incidence angles caused by curvature variations of the profiles. Absolute yields are computed by Eq. (2) using the semi-empirical relationships of Matsunami and Yamamura et al. [17], which are regarded as more accurate than the previously reported Sigmund model.

$$S(\theta) = St^f e^{-\sum(t-1)} \quad (2)$$

where $t=1/cos(\theta)$, f is the mass ratio of the projectile/target, and S is the sputter yield at normal incidence. The method has the following drawbacks: fabrication error caused the profile error to be large, especially profiles with large depth; and, large memory space is required. Figure 1(a) illustrates the method through which the surface erosion speed v can be calculated by Eq (1). However, for a real continuous surface, the surface erosion/deposition takes place along the normal direction (speed n in Figure 1(a)) [18-21]. This causes error and deviation from the predefined shape.

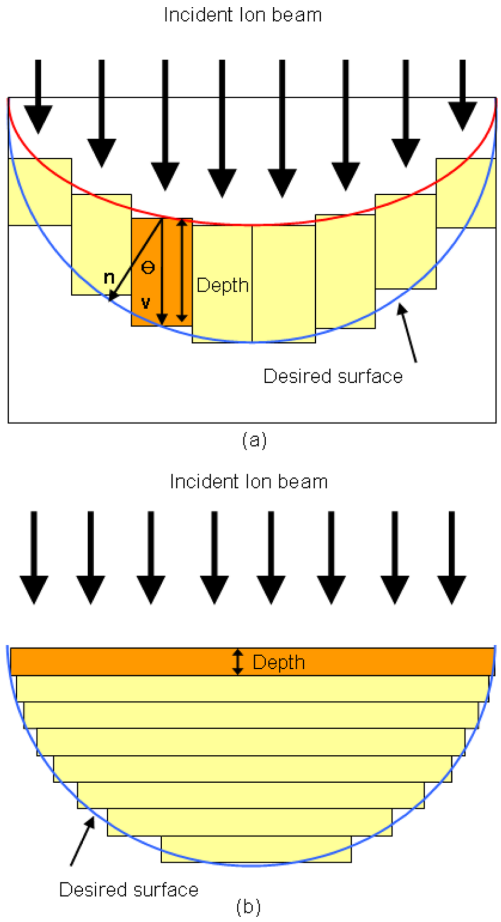

Figure 1. Schematic illustration of Vasile's depth control method (a) and Fu's slice by slice layer method (b).

2. Slice by Slice approach

This method is used to transfer the desired 3D cavities to many discrete 2D flat slices. In other words, many sequential 2D slices with small thicknesses are used to approach the desired 3D cavities. Then, the milling of the 3D structures can be and used to mill many sequential 2D flat slices instead of the reported Vasile cavities. This is the apparent difference between the Slice by slice method and Vasile's depth control method. For the total number of slices N, the total number of milling steps N is needed. Therefore, in this method, the sputter yield and the dwell times are constants for milling the flat slices, instead of changing sputtering yield and dwell time at each pixel.

For the formation of a certain cavity by FIB milling, Fu transferred the structure to the discrete 2D slices with total number N according to the maximum depth of the parabolic cavity; each slice has the same thickness. The

smooth sidewall profile transition permits the milled pixel addresses of the next slice to be different. In that way, the bottom of the milled crater (the boundary between two slices) is a plane near the flat surface. For this reason the mean sputtering yield can be assumed to be a constant and can be calculated for the case of vertical ion bombardment. Because the slices are flat in 2D, the sputter yield and dwell time are constant on surfaces other than the pixels at the periphery of the slices, for which the sputter yield is different from that of the other slices due to variation of the normal direction at the periphery of the slices, which causes varying of the beam incident angles at the sidewall of the parabolic cavity. This method is illustrated in Figure 1(b); depths of each slice are calculated using Eq. (3).

$$\Delta Z = \frac{St}{\eta}\iint \phi(x,y) f_{x,y}(x_i, y_j)\,dx\,dy \tag{3}$$

However, the method has the following drawbacks: surface roughness at both the right and left sides of each layer because of the beam tail; redeposition flux was not considered; and it is difficult to consider redeposition at this step However, this method was found to be very applicable to features that have small aspect ratio.

3. Multi surface driving method (MSDM)

We will now discuss the multiple surface driving method, which starts with a predefined structure, as shown in Figure 2. The last shape in the figure is the goal of the fabrication; the layer between the initial layer and the last layer is an equally divided virtual layer. Simply, the depth of the last shape is divided into an integer number of slice layers N. The beam is then placed above the structure and can be configured with the process parameters such as the number of pixels, pixel spacing (or pixel overlap), dwell time and number of passes. Total current density above the surface can be configured using those process parameters so that each layer can be fabricated. For example, the current density of point A can be calculated along the dotted line. At each layer, the surface driving power (or current density) can be calculated if the travel distance of the two neighboring surfaces is known. In the previously mentioned paper by Adams and Vasile, the surface travel distance was calculated using the depth. However, according to the well-established surface erosion model, the surface moves along the normal direction, not the z direction (direction of depth). The surface erosion is modeled using Huygens wavefront construction in Eq. (1); for this process, all surface points on the wavefront advance by a certain distance d, in the normal direction, in a given time t, expressed by Eq. (4).

$$d_{normal} = J(x)Y(\theta)t/N \tag{4}$$

Here z is the direction of the incoming ion beam and x is the spatial co-ordinate perpendicular to z; N is the atomic density, and $J(x)$ is the ion flux, which depends on the spatial x co-ordinate. $Y(\theta)$ is the sputtering yield (atoms per ion) and θ is the ion beam incident angle.

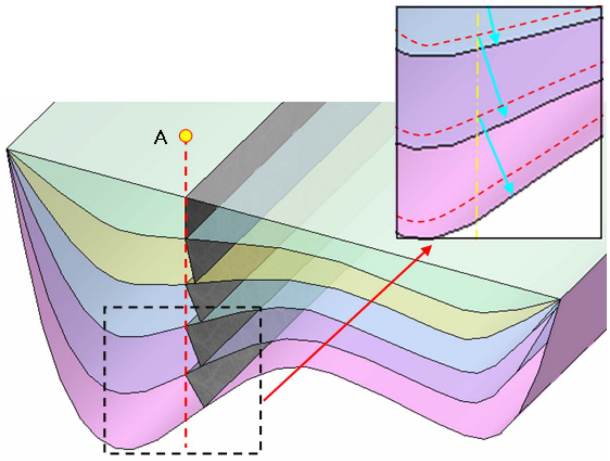

Figure 2. Schematic illustration of surface driving method. The arrows indicate the normal direction and the distance between two equally sliced neighboring layers. The dotted lines in the inset indicate the redeposited layer at each sliced surface.

The normal direction and the distance between each layer are expressed by arrows in the small inset (in Figure 2); the distances along the x- (dx) and z-directions (dz) are also calculated using Eqs. (5) and (6), respectively, which are derived from Eq. (4):

$$d_x N = J(x)\cos(\theta)\sin(\theta)Y(\theta)dt \tag{5}$$

$$d_z N = J(x)\cos^2(\theta)Y(\theta)dt \tag{6}$$

Calculated surface driving distance d can be used to calculate the total current density profile $J(x)$. This is the main idea of the MSDM. Furthermore redeposition flux will retract the surface in the opposite direction of the erosion direction. For a consideration of the redeposition, the surface travel distance can be calculated from the redeposited layer (in Figure 1). The redeposition flux is determined at a certain surface point using the integral of all the contributions of the sputter fluxes originating from other positions along the surface [14-16]. If the surface is composed of small flat pieces, as in the case of Vasile, or is fully flat, as in the case of Fu, as shown in Figure 1, Eqs. 5 and 6 can then correspond to Eqs. 7 and 8:

$$d_x N = 0 \tag{7}$$

$$d_z N = J(x)Y_o dt \tag{8}$$

Here, Y_0 is the sputtering yield at normal incidence. In other words, an assumption that the surface is flat can be useful for simple calculation or surface fabrication with Eqs. 7 and 8.

This method is based on a sound mathematical concept,

and therefore is very suitable for the fabrication of predefined features. In addition to the mathematical concept, the redeposition flux is naturally considered in MSDM.

4. Single surface driving method (SSDM)

In MSDM, multiple layers are used to fabricate a desired structure. Each sliced layer uses a corresponding ion dose profile. However, if there are many layers, such that the distance between two layers becomes small, the differences between each ion dose profile become smaller. This means that all the ion dose profiles are similar. This is the concept behind the single step surface driving method (SSDM). This method relies on simple mathematical approximation, whereas MSDM is based on a strong mathematical background. Therefore, only one ion dose profile is used in SSDM, which leads to an advantage for ion dose profile preparation, saves storage space for stream files and eases the fabrication of the machine with just one stream file. So, SSDM is practical in comparison to MSDM. Multiple ion dose profiles can be converted into just one profile in several ways; however, in this paper, only the average ion dose profile among multiple ion dose profiles is used.

III. Experiments

Experiments were carried out using an FEI NOVA 200 Dualbeam system equipped with a Gallium liquid-metal ion source (LMIS) and scanning electron microscope (SEM). The experiments were performed at an acceleration voltage of 30 kV and a beam current of 9.7 pA. For experimental convenience, the fabrications were made near the edge of the sample so that additional processes such as cross sectioning and deposition were not necessary. After fabrication, the cross sections were investigated with scanning electron microscopy perpendicular to the cross section of the fabricated shape. Three-dimensional structures were modeled with commercially available computer aided design (CAD) software Solidworks [22] and saved in stereolithography file format (.stl extension) [23]. The STL file describes a raw unstructured triangulated surface by the unit normal and vertices of the triangles in 3D space.. A special program code has been made so that the stored stereolithography file can be loaded, sliced into several layers. The current density profile was calculated using the concept of variable dwell time for each layer and profile was summarized for one layer. The pixel dwell times are stored, as well as the pixel positions, in a file called a stream file, which is the input for the FIB machine. The scanning was reordered such that all the pixels had the same pixel dwell time; otherwise, the shape will be different from the desired one [24].

IV. Results and Discussion

1. Fabrication of defined structures

For the fabrication of the predefined curved structure (see Figure. 1), the average ion dose profile is calculated using 100 layers and shown in Figure 3; the five ion dose profiles used in MSDM for the same free-curved structure

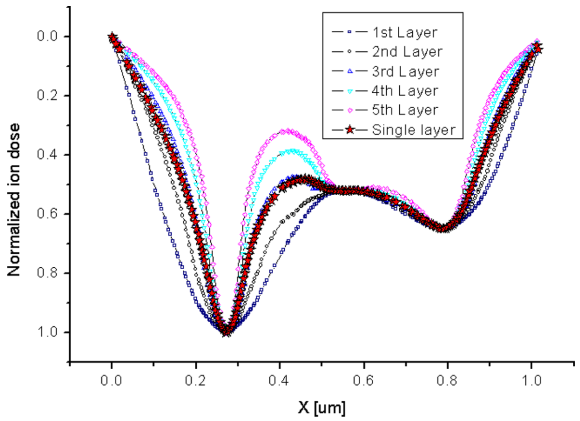

Figure 3. Normalized ion dose profiles for a predefined free curve. The single layer represents by a layer using 100 layers. the others represent the five ion dose profiles used in MSDM with the five layers.

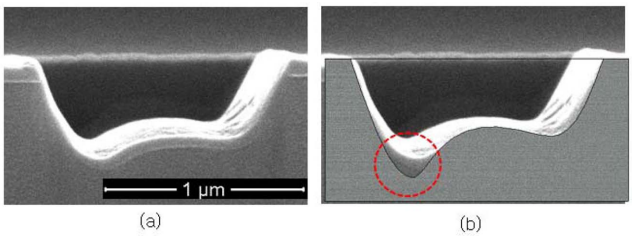

Figure 4. SEM images of fabricated predefined free curved structure; final shape (a) and predefined shape overlap with final shape (b). The left side wall and bottom pit on the left are slightly different from the desired shapes because the sample stage is rotated slightly. Red-dotted circle indicates deviation between the desired and the fabricated shapes.

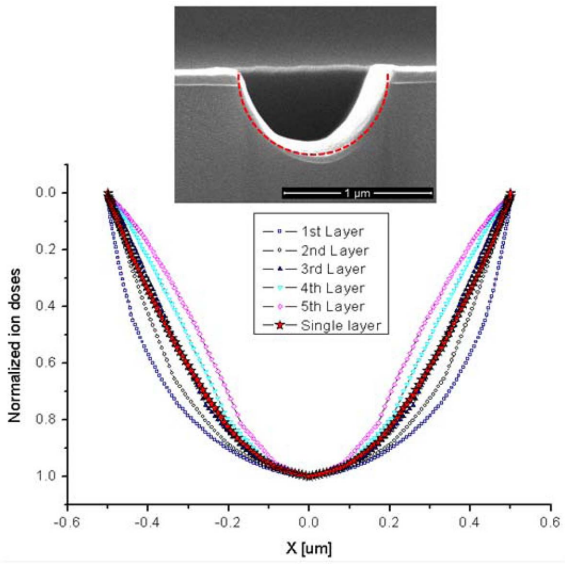

Figure 5. Normalized ion dose profiles for circular curve. The single layer represents the average of 100 layers and the others represent the five ion dose profiles used in the MSDM with five layers. The inset is an SEM image of the fabricated circular pattern. Red-dotted curve indicates desired half-circle.

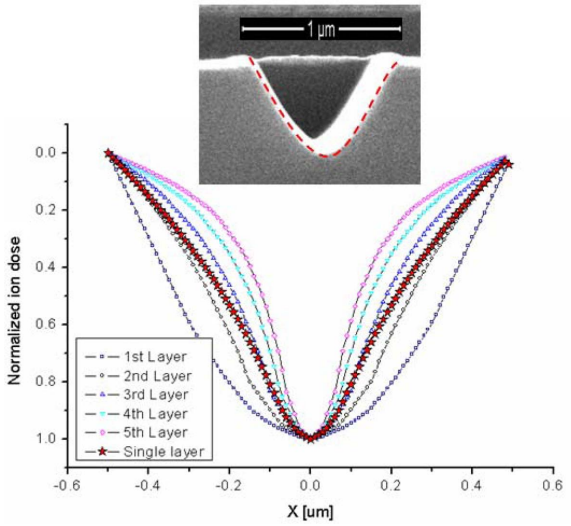

Figure 6. Normalized ion dose profiles for parabolic curve. The single layer represents the averaged of 100 layers and the others represent the five ion dose profiles used in MSDM with five layers. The inset is an SEM image of the parabolic structure. (Maximum depth of the structure is 550 nm). Red-dotted curve indicates desired parabolic shape.

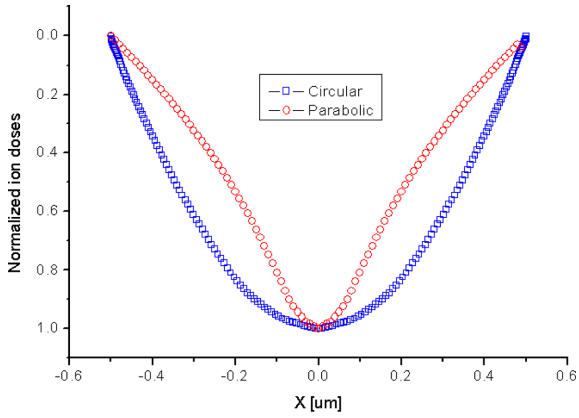

Figure 7. Comparison of optimized ion dose profiles for both circular and parabolic structures.

were also calculated . The SSDM ion dose profile is similar to the 3rd ion dose profile used in MSDM; the corresponding fabricated free curved structures at different numbers of passes are shown in Figure 4.

Fabricated circular structure is shown in Figure 5, as well as multiple and single ion dose profiles.

For comparison of the ion dose profiles, those of circular and parabolic structure are shown in Figure 7. As expected, the bowl width of the circular ion dose profile is much larger than those of the parabolic profile. However, the ion dose profiles are not similar to the final shape of the structures, either circular or parabolic, because the surface moves along the normal direction.

2. Verification by simulation

To verify the SSDM, computational simulations were performed for the two ion dose profiles, for the circular and parabolic features, with results shown in Figure 7. The

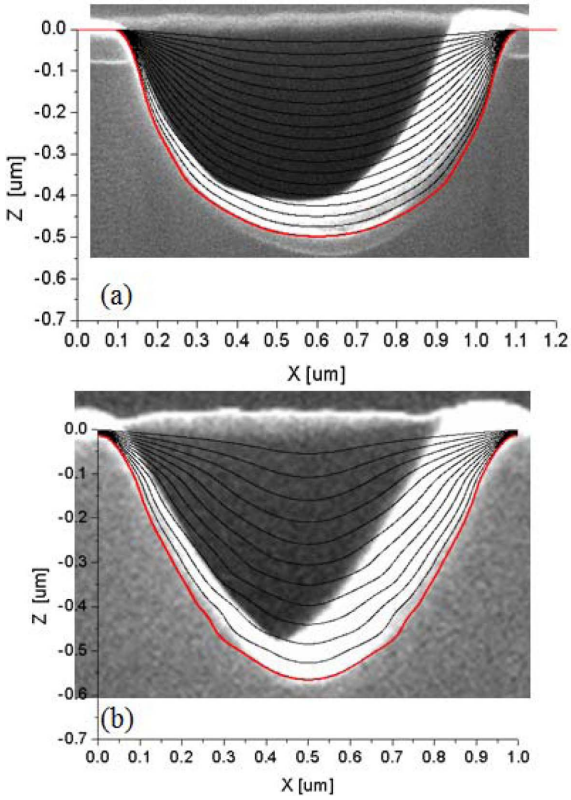

Figure 8. Simulation results of (a) circular and (b) parabolic structures. Results overlap with experimentally obtained structures.

simulation method and related model are exactly described in the literature [25-27]. In the simulation, the ion dose profiles are used as input; the final simulation results should be similar to the desired shape if the SSDM is suitable for the fabrication of predefined features. The simulation results for the circular and parabolic shapes are shown in Figures 8(a) and (b), respectively. The two results overlap with experimentally obtained structures. These results show that the two fabricated structures are in good agreement with the simulated results.

V. Summary

For the accurate fabrication of predefined structures, two useful methods have been developed: the Slice by slice method and the variable dwell time control. However, neither of them considers the redeposition of sputtered particles. For a consideration of the redeposition, MSDM is here reported. However, MSDM uses multiple ion dose profiles for one desired structure, and so the processes are somewhat complicated despite their accuracy and mathematical stability. For simplicity of the fabrication process, the Single step surface driving method (SSDM) is used; this method utilizes one optimized ion dose profile.

SSDM is used for the fabrication of predefined free curved structures, and for circular and parabolic structures. The fabricated structures were compared to the simulation

results and were found to be in in good agreement. Single step surface driving has an advantage compared to multi step surface driving for the preparation of the ion dose profile and the corresponding stream file preparation. SSDM is particularly useful in modern digitally controlled FIB machines. Saving of processing time and simplicity of process can be achieved using SSDM without great loss of accuracy. The method can be useful for fabricating structures and in various applications [28,29].

References

[1] R. D. Purdr. Appl. Optics 3, 167 (1994).
[2] V. Kudryashov, X. C. Yuan, W. C. Cheong, and K. Radhakrishnan, Microelectron. Eng. 67, 306 (2003).
[3] S. Maruo, O. Nakamura, and S. Kawata, Opt. Lett. 22, 132 (1997).
[4] V. A. Kudryashov and S. Lee, Microelectron. Eng. 57, 819 (2001).
[5] K. K. Seet, V. Mizeikis, S. Juodkazis, and H. Misawa. J. Non-Cryst. Solid. 352, 2390 (2006).
[6] D. Resnick, S. V. Sreenivasan, and C. G. Willson, Material Today 8, 34 (2005).
[7] C. M. Waits, A. Modafe, R. Ghodssi, and J. Micromech. Microeng. 13, 170 (2003).
[8] J. Pietarinen, S. Siitonen, N. Tossavainen, J. Laukkanen, and M. Kuittinen, Microelectron. Eng. 83, 492 (2006).
[9] C. Ochiai, O. Yavas, M. Takai, A. Hosono, and S. Okuda, J. Vac. Sci. Technol. B 19, 933 (2001).
[10] Y. Fu and N. K. A. Bryan, J. Vac. Sci. Technol. B 22, 1672 (2004).
[11] Y. Fu and N. K. A. Bryan, IEEE T. Semiconduct M. 15, 229 (2002).
[12] D. P. Adams and M. J. Vasile, J. Vac. Sci. Technol. B 24, 836 (2006).
[13] D. P. Adams, M. J. Vasile, and T. M. Mayer, J. Vac. Sci. Technol. B 24, 1766 (2006).
[14] H. B. Kim, G. Hobler, A Steiger, A Lugstein, and E. Bertagonolli, Opt. Express 15, 9444 (2007).
[15] H. B. Kim, Microelectron. Eng. 88, 3365 (2011).
[16] H. B. Kim, Microelectron. Eng. 91, 14 (2012).
[17] N. Matsunami, Y. Yamamura, Y. Itakawa, N. Itoh, Y. Kazumata, K. Miyagawa, K. Morita, and R. Shimizu. Nagoya University, IPPJ-AM-14. (1980).
[18] R. Smith, S. J. Wilde, G. Carter, I. V. Katardjiev, and N. J. Nobes, J. Vac. Sci. Technol. B 5, 579 (1986).
[19] I. V. Katardjiev, J. Vac. Sci. Technol. A 6, 2434 (1988).
[20] I. V. Katardjiev, J. Vac. Sci. Technol. A 7, 3222 (1989).
[21] I. V. Katardjiev, G. Carter, M. J. Nobes, S. Berg, and H. O. Blom, J. Vac. Sci. Technol. A 12, 61 (1993).
[22] Solid works Manual http://www.solidworks.com. Dassault system (2008).
[23] Wikipedia, http://en.wikipedia.org/wiki/STL_(file_format)
[24] S. Cabrini, C. Liberale, D. Cojoc, A. Carpentiero, M. Prasciolu, S. Mora, V. Degiorgio, F. Angelis, and E. D. Fabrizio, Microelectron. Eng. 83, 804 (2006).
[25] H. B. Kim, G. Hobler, A. Lugstein, E. Bertagonolli, and J. Micromech. Microeng. 17 1178 (2007).
[26] H. B. Kim, G. Hobler, A. Steiger, A. Lugstein, and E. Bertagonolli, Nanotechnology 18, 245303 (2007).
[27] H. B. Kim, G. Hobler, A Steiger, A Lugstein, and E. Bertagonolli, Nanotechnology 18, 265307 (2007).
[28] S. Lee and D. -G. Kim, Applied Science and Convergence Technology, 24, 162 (2015).
[29] E. B. Cho, H. M. Kwon, H. S. Lee, and J.-S. Yeo, J. Kor. Vac. Soc. 22, 262 (2013).